

CONF 890665-2

PHOTOCONDUCTIVE SEMICONDUCTOR SWITCH (PCSS) RECOVERY\*

F. J. Zutavern, G. M. Loubriel, B. B. McKenzie, W. M. O'Malley,  
R. A. Hamil, L. P. Schanwald, H. P. Hjalmarson  
Sandia National Laboratories  
Albuquerque, New Mexico 87185

Received by OSTI

JUN 05 1989

Abstract

SAND--88-3356C

DE89 012657

Attempts to use photoconductive semiconductors as high-power (10-100 kV, 0.1-2 kA) toggling switches with recovery times of 5-100 ns have stimulated the exploration of their recovery mechanisms. We have observed that optically triggered GaAs switches exhibit "lock-on," i.e., when triggered, they do not recover as long as they are holding more than 4-8 kV/cm. Experiments are being performed to determine the minimum recovery time of these switches after lock-on, by immediately reducing their fields or currents. As an alternative to GaAs, Si is a semiconductor that does not exhibit lock-on. It has a very long recovery time ( $\geq 100 \mu s$ ) that can be shortened to less than 100 ns with highly concentrated gold doping ( $\geq 10^{15}/cm^3$ ). Device models that predict the behavior of PCSS and experiments on the recovery of GaAs and Au:Si switches are presented.

Introduction

The significance of the fast closing properties of PCSS for pulsed power applications is discussed in the literature.<sup>1-4</sup> Fast-recovery, high-power switches are also needed for many applications from 1 kHz to 1 GHz, because this frequency is beyond the realm of reasonable operation for spark gaps. This paper concentrates on the opening properties of PCSS and is, therefore, relevant to fast recovery or high frequency pulsed power switching applications.

At moderate fields (below 4-12 kV/cm depending on the type of sample), semiconductors, such as GaAs or InP, exhibit sub-nanosecond carrier recombination. Hence, the photo-resistance of switches made from these materials recovers from the on-state in a few nanoseconds after the triggering light pulse ends. We have switched GaAs at voltages in excess of 100 kV (67 kV/cm), and larger switches can be made to handle proportionately higher voltages. The amount of light energy required to trigger such switches in a fast recovery mode, however, makes them impractical for many applications. (Our 1-in. diameter chrome-doped GaAs switches require  $\sim 30 \mu J$  to reach  $5 \Omega$  for 10 ns. These have switched 46 kV, 800 A in a  $50 \Omega$  test system.)

This report was prepared as an account of work sponsored by an agency of the United States Government. Neither the United States Government nor any agency thereof, nor any of their employees, makes any warranty, express or implied, or assumes any legal liability or responsibility for the accuracy, completeness, or usefulness of any information, apparatus, product, or process disclosed, or represents that its use would not infringe privately owned rights. Reference herein to any specific commercial product, process, or service by trade name, trademark, manufacturer, or otherwise does not necessarily constitute or imply its endorsement, recommendation, or favoring by the United States Government or any agency thereof. The views and opinions of authors expressed herein do not necessarily state or reflect those of the United States Government or any agency thereof.

**DISCLAIMER**

DISTRIBUTION OF THIS DOCUMENT IS UNLIMITED

**MASTER**

## **DISCLAIMER**

**This report was prepared as an account of work sponsored by an agency of the United States Government. Neither the United States Government nor any agency thereof, nor any of their employees, makes any warranty, express or implied, or assumes any legal liability or responsibility for the accuracy, completeness, or usefulness of any information, apparatus, product, or process disclosed, or represents that its use would not infringe privately owned rights. Reference herein to any specific commercial product, process, or service by trade name, trademark, manufacturer, or otherwise does not necessarily constitute or imply its endorsement, recommendation, or favoring by the United States Government or any agency thereof. The views and opinions of authors expressed herein do not necessarily state or reflect those of the United States Government or any agency thereof.**

---

## **DISCLAIMER**

**Portions of this document may be illegible in electronic image products. Images are produced from the best available original document.**

At high fields (above 4-12 kV/cm, depending on the type of sample), both GaAs and InP exhibit lock-on. This mode of switching will be discussed in more detail later in this paper. The two most important features of lock-on are: (1) As the name implies, once triggered, the switch stays on until the field is reduced below a threshold. (2) The light energy required to trigger a switch into lock-on is much less (~1/500th) of that required to activate the switch at low fields (normal, linear photoconductivity). It is this second feature, a significant trigger gain, that makes PCSS attractive to more applications.

At a glance, one might think that a switch that locks-on would be useless for fast recovery applications. However, the importance of a switching mode with trigger gain has led us to try to understand lock-on. We are trying to determine what keeps these switches from recovering at high fields. By developing a model for lock-on behavior, we have been able to design and test circuits that trigger a PCSS into lock-on and then induce fast recovery by reducing the switch fields or currents temporarily. In this way, we hope to circumvent the lock-on problem and take advantage of its trigger gain to produce a class of high frequency, low trigger energy devices.

### Linear Photoconductivity

With normal, linear photoconductivity, one electron-hole pair is created for each photon absorbed in the semiconductor. If  $N$  is the total number of photons absorbed in a switch of volume  $LA$ , then the resistance of the switch is given by

$$\frac{1}{R} = \sigma \frac{A}{L} = \frac{Ne\mu}{L^2}, \quad (1)$$

where  $\sigma$  is the photo-induced conductivity,  $L$  is the length of the switch parallel to the current,  $A$  is the cross-sectional area of the sample perpendicular to the current,  $e$  is the charge of an electron,  $\mu$  is the carrier mobility (electrons and holes averaged). Carriers created by absorbed photons eventually recombine at a rate characteristic of the semiconductor. If this rate depends on the concentration of only one type of carrier, then carriers disappear exponentially in time. This is clearly the case in Au:Si shown in Fig. 1. The resistance of the switch, that was derived from the ratio of measured switch voltage to current, increases with a 14-ns exponential time constant. If  $I(t)$  represents the number of photons absorbed per unit time from the activating light pulse as a function of time, then the number of photo-carriers at any point in time is given by

$$N(t) = \int_{-\infty}^t I(s) e^{(s-t)/(\tau_R)} ds . \quad (2)$$

For light pulses much narrower than the carrier recombination time,  $\tau_R$ , Eq. (2) reduces to simple exponential decay. This is illustrated in Fig. 1 as an exponential increase in resistance. On the other hand, for light pulses much wider than  $\tau$ , the carrier concentration is simply proportional to the light intensity. This is the case for Cr:GaAs shown in Fig. 2. Here, the voltage and current through the switch have the same shape as the laser pulse that activated the switch. The voltage across the GaAs switch did not drop as close to zero as the Au:Si switch, because less light intensity was used with the GaAs.

### Lock-On

At high fields, GaAs and InP switches operate in a mode that we call lock-on. Switching waveforms and characteristics of this mode have been described in previous papers.<sup>5-7</sup> Here, we summarize the physically observed properties of these switches and show voltage, current, and light trigger waveforms for one example in Fig. 3. In this example, the switch is pulse charged to -32 kV across a 1.5 cm- long, 2-cm wide switch. When the laser fires, the voltage drops to 12 kV and the current increases to 400 A. These levels remain relatively constant until the energy has been dumped from the charging system (160 ns from trigger) and the voltage and current drop to zero. lock-on, illustrated in this figure, is in contrast to the normal linear photoconductivity discussed above and illustrated in Fig. 2.

The characteristics of this lock-on switching mode are summarized below:

1. The field across the switch must be higher than the lock-on field (3.6 kV/cm for our purest GaAs, 8.5 kV/cm for Cr:GaAs, and 14.4 kV/cm for Fe:inP).
2. Light triggering is required. The switches do not apparently go into lock-on from the thermal carriers in the dark. We have pulse charged GaAs to 140 kV/cm without triggering for 2-5  $\mu$ s and dc-charged to 30 kV/cm for several minutes without observing significant conduction.
3. Lock-on can be triggered using ~1/500th the amount of light required to switch the same samples at low fields (linear photoconductivity). There is a gain mechanism involved with lock-on.

4. Upon triggering, the field across the switch drops to the lock-on field and the current passed is whatever the circuit will supply while maintaining the lock-on field across the switch. We have tested loads ranging from  $< 1 \Omega$  to  $50 \Omega$ .
5. The resistance of the switch recovers when the field is reduced below a characteristic threshold.

The remainder of this paper discusses this recovery and the rate at which it occurs. Issues are: whether the switch will recover when its carrier density decreases below that required for triggering; how the time required for recovery is related to the carrier recombination time at low fields; and whether some other characteristic times enter into the problem.

### Physical Models

There have been several possible explanations offered for the lock-on switching mode. One of these involves impact ionization of deep level traps. It is discussed in a companion paper on closing PCSS presented at this conference.<sup>8</sup> A second explanation predicts the creation of multiple charge domains at high fields due to the negative differential resistivity of GaAs, which is also responsible for the Gunn effect.<sup>9</sup> This second explanation is offered here because it fits the physically observed features of lock-on and gives valuable insight into the device modeling discussed below. In fact, the most appropriate explanation for lock-on may be a combination of these phenomena and others that we have not mentioned.

Shortly after lock-on switching was first observed, it was pointed out that the field onto which our GaAs switches appeared to lock was slightly higher than the threshold field for the Gunn effect,<sup>9</sup> that is 3.2 kV/cm for very pure GaAs. With higher concentrations of impurities this field increases. Indeed, our purest samples showed the lowest lock-on field, ~3.6 kV/cm, and our most heavily doped samples showed ~8.5 kV/cm. In small devices,  $\leq 100 \mu\text{m}$  long, the Gunn effect leads to high frequency oscillations. Our 1.5-cm long switches show some small, but persistent oscillations lasting more than 100 ns in time (Fig. 3). However, the Gunn effect alone would not explain the apparent trigger gain exhibited by our switches.

In most solids, the velocity of charge carriers increases linearly with field, until about  $10^7 \text{ cm/s}$ , where it begins to saturate due to increased scattering of the carriers. GaAs is unusual in that at high fields its carrier velocity not only saturates, but starts decreasing with increasing fields. This produces a situation with negative differential resistivity.

allowing for the growth of negative charge domains that move across the sample from the cathode to the anode. In fact, Poisson's equation and an expression for the current in one dimension can be used to show that the impedance of the sample will vanish when the carrier concentration,  $n$ , times the length of the sample,  $L$ , is a critical value

$$nL = 3 \times 10^{11} \text{ cm}^{-2}, \quad (3)$$

for n-type GaAs with a negative differential mobility of  $500 \text{ cm}^2/\text{Vs}$  at  $10^7 \text{ cm/s}$ .<sup>10</sup> For a given sample length, there is a minimum carrier concentration for the formation of domains. At higher carrier concentrations or longer lengths multiple domains are formed.<sup>10</sup> Since the dark carrier concentration of our 1.5-cm long switches is  $10^9\text{-}10^{10}/\text{cm}^3$  (derived from the dark resistance), domains cannot form until additional carriers are supplied.

A single charge domain, traveling at  $10^7 \text{ cm/s}$ , will traverse our 1.5-cm samples in 150 ns. The existence of higher frequency oscillations ( $\sim 160 \text{ MHz}$ ) suggests the formation of multiple domains  $\sim 0.6 \text{ mm}$  apart. (This, incidentally, is the thickness of our switches perpendicular to the current flow, which may be a coincidence, or may be affecting the size of the domains.) Along with charge domains come electric field domains due to the local imbalance of carrier and donor charge. This model requires that the electric field at the peak of these domains is sufficient to cause avalanche carrier generation (100-200 kV/cm). At sufficient average field, a low light level trigger pulse supplies the critical carrier concentration for multiple domain growth. Then avalanching produces the carriers that explain the trigger gain. If too many carriers are created, the resistance of the sample drops too low for the circuit to supply the lock-on field across the switch. Then the domains disappear and normal carrier recombination occurs. Evidence for such high field domains has been given for samples that were doped heavily enough to reach the critical carrier concentration without laser triggering.<sup>11,12</sup>

#### Device Model

In order to design circuits with lock-on switching, a device model was needed. This model had to calculate the switch resistance for a simulation code at each time step of the calculation. Given the voltage across the switch and its previous resistance, an approximation for its new resistance was calculated. Since the resistance,  $R$ , of the switch is inversely proportional to the total number of carriers,  $N$ , in the switch,

$$\Delta R = \frac{dR}{dN} \Delta N = - \frac{R}{N} \Delta N . \quad (4)$$

An estimate for the change in number of carriers was calculated based on exponential recombination time,  $\tau_R$ , total photons absorbed per unit time,  $I(t)$ , and exponential carrier generation time,  $\tau_L$ .

$$\frac{dN}{dt} = - \frac{N}{\tau_R} + I(t) + \frac{N}{\tau_L} \left\{ \begin{array}{l} V \geq V_L \\ N \geq N_L \end{array} \right\} . \quad (5)$$

The last term is included only at times when the voltage,  $V$ , across the switch exceeds the lock-on voltage,  $V_L$ , and the total number of carriers,  $N$ , exceeds a critical number of carriers,  $N_L$ . In other words, this model assumes normal carrier recombination if the switch field or carrier density is below the critical values required for lock-on. If these values are both exceeded, then provided  $\tau_L$  is shorter than  $\tau_R$ , the carrier concentration will increase until the switch voltage is limited by the circuit. This model was used to simulate lock-on (Fig. 4) and its recovery for the circuits described in the following sections.

#### Field Reducing Reflections

The circuit shown in Fig. 5 was devised and tested to induce switch recovery after lock-on. This circuit gives the switch some time to recover by reducing the field below lock-on for a few tens of nanoseconds after it has been triggered. A simulation of this circuit is shown in Fig. 6. The switch voltage and current from a successful test using a 1-in. diameter Cr:GaAs switch are shown in Fig. 7. When the switch, initially charged to 26 kV, is triggered with a  $\geq 1.5\text{-mJ}$ , 10-ns wide, 532-nm laser pulse, its voltage drops to the lock-on voltage,  $V_L = 13$  kV (like a "triggered Zener diode"). At this point, it drives the load resistor and charges the transmission line to  $V - V_L = 13$  kV. A reflection from the transmission line increases the voltage across the load (while the switch is on) to about 20 kV, leaving only 6 kV across the switch for the next 26 ns. Since this is below the lock-on threshold, the carriers in the switch recombine and the switch recovers its resistance as shown by the switch current in Fig. 7. The result is a 50-60 ns wide voltage pulse and a 30-ns wide current pulse.

Comparison of the simulation (Fig. 6) and the data (Fig. 7) show reasonable agreement in the prediction of recovery, the lock-on level, and the time and magnitude of the voltage reflections. The data show a slower fall to lock-on and a longer recovery. This may indicate a smaller

difference between  $\tau_R$  and  $\tau_L$  than was used as a test in the simulation (2 ns and 1 ns, respectively). It might also be evidence for a more gradual dependence of carrier generation on the field near lock-on rather than the step function dependence indicated in Eq. 5.

The difference between recovery and no-recovery is illustrated in Figs. 8 and 9. In both cases, the switch was triggered into lock-on. However, in Fig. 9 the switch triggered with 1.5 J of 532-nm light recovered, and the switch triggered with 1.4 mJ did not. Repeated tests at a variety of laser pulse energies showed recovery for all shots  $\geq 1.5$  mJ, and, surprisingly, no recovery for lower energies. Since the model does not predict a minimum trigger level for recovery, it is possible that a more complicated model is required. On the other hand, it was noted that higher energy shots appeared to have a somewhat sharper fall to lock-on that resulted in a slightly larger reduction in the field across the switch due to the reflection. So the circuit may simply work better when the switch is triggered with higher laser energies.

#### Current-Limiting Transmission Line

An alternative to reducing the field across the switch is to limit the current through the switch after lock-on. Since the switch must obey Ohm's Law instantaneously, limiting the current will produce either a smaller voltage drop across the switch or a higher resistance. Once the resistance has increased above the critical value for lock-on, the switch may recover.

Figure 10 shows a circuit that abruptly limits the switch current once a transmission line is charged. The load, in series with the switch and the transmission line, will pass current and see half the circuit voltage until the transmission line is charged. After the switch has been given some time to recover, a second switch is used to discharge the transmission line to ground. This produces a bipolar pulse on the load, changing the direction of current flow and restoring the voltage drop across the first switch (less the lock-on voltage drop across the second switch). The advantage of this circuit over the previous one is that it delivers a narrower pulse to the load that is free from the voltage reflections produced in the first circuit. A simulation of this circuit, that uses the device model for lock-on discussed above, is shown in Fig. 11. The voltage across the first switch shows a spike when the transmission line has charged, 26 ns after triggering. When the second switch is triggered at 40 ns, the first switch has recovered. It now holds the initial voltage less the lock-on voltage drop.

#### Inductively Limited Current

Another way to enhance recovery from lock-on, which limits the current through the switch over longer periods of time, is simply to limit the recharge rate of a fast storage element. Figure 12 shows an inductively limited charging circuit for a transmission line that is discharged rapidly through a PCSS. To determine whether the switch will recover from lock-on, the rate of increase in the current is limited to less than the switch can handle, while maintaining the lock-on voltage and critical triggering resistance.

After the transmission line has been discharged, the maximum rate of current increase through the switch is given by the available voltage divided by the limiting inductance,  $L$  (not to be confused with length). An upper limit to the voltage across the switch is given by

$$IR = \left( \int \frac{dI}{dt} dt \right) R < \frac{(V-V_L)}{L} \tau R_L e^{-t/\tau} < \frac{(V-V_L)}{L} \tau R_L , \quad (6)$$

where  $R$  is the switch resistance,  $R_L$  is the resistance required to trigger lock-on, and  $L$  is the current-limiting inductance. The switch voltage is guaranteed to be less than the lock-on voltage when the right-hand side of relation 6 is less than the lock-on voltage or

$$\frac{(V-V_L)}{V_L} \tau R_L < L . \quad (7)$$

The mode predicts recovery will occur whenever the current-limiting inductance is greater than the left-hand side of relation 7. A simulation of this situation is shown in Fig. 13. This circuit has been assembled and will be tested in the near future.

### Conclusions

The lock-on switching mode for PCSS was described and a possible phenomenological explanation was suggested. The physically observed features of lock-on were incorporated in a device model. The model was used to simulate recovery and experimental data verified that prediction for one circuit demonstrating recovery in less than 30 ns. Other circuits were described that induced fast recovery from lock-on when simulated. This paper shows that the trigger gain from lock-on can be used advantageously in applications that still demand fast recovery.

Future work will include more tests of simulated circuits to determine the accuracy and usefulness of this model. Other measurements will also be made to try to understand

more fundamental initiation and recovery mechanisms of lock-on.

### References

1. G. M. Loubriel, M. W. O'Malley, and F. J. Zutavern, in Proceedings of 6th IEEE Pulsed Power Conference, Arlington, VA, 1987, 145.
2. F. J. Zutavern and M. W. O'Malley, in Proceedings of 17th IEEE Power Modulator Symposium, Seattle, WA, 1986, 214.
3. W. C. Nunnally, in Proceedings of 5th IEEE Pulsed Power Conference, Arlington, VA, 1985, 235.
4. C. H. Lee (ed.), Picosecond Optoelectronic Devices, (Academic Press, NY, 1984).
5. F. J. Zutavern, et al., in Proceedings of the 18th IEEE Power Modulator Symposium, Hilton Head, SC, 1988, 307.
6. F. J. Zutavern, M. W. O'Malley, and G. M. Loubriel, in Proceedings of 6th IEEE Pulsed Power Conference, Arlington, VA, 1987, 577.
7. G. M. Loubriel, et al., to be submitted to Appl. Phys. Lett., 1989
8. G. M. Loubriel, et al., in Proceedings of the 7th IEEE Pulsed Power Conference, Monterey, CA, 1989.
9. J. B. Gunn, IBM Journal, April, 141, 1964.
10. K. Seegar, Semiconductor Physics, (Springer-Verlag, NY, 1982) 232-245.
11. J. S. Heeks, IEEE Transactions on Electron Devices, ED-13, 68, 1966.
12. M. Ohtomo, Jpn. J. of Appl. Phys., 7, 1969, p. 1368.

---

\*This work was supported by the U.S. Department of Energy under Contract DE-AC04-76DP00789.

### Figure Captions

Figure 1. Measured V/I for a Au:Si PCSS triggered with a 10-ns wide laser pulse at  $1.06 \mu\text{m}$ . The exponential fit shows a 14-ns carrier recombination time.

Figure 2. Voltage, current, and laser waveforms for a 1-in. diameter Cr:GaAs switch triggered with a 532-nm laser pulse at moderate voltages (below lock-on).

Figure 3. Voltage, current, and laser waveforms for a 1-in. diameter Cr:GaAs switch triggered with a 532-nm laser pulse at high voltages (above lock-on). Although the laser pulse is only 10-ns wide, the switch stays on for 160 ns, at which time the storage line energy has been completely dissipated.

Figure 4. *Voltage waveforms series*  
Input, switch, and load voltages for an L-R-C circuit switched into lock-on. The slow rise in the load voltage is due to the inductance in this circuit. These curves were obtained using the device model for lock-on described in the text.

Figure 5. The circuit used to induce recovery from lock-on, by reducing the voltage across the switch with a reflection from a transmission line.

Figure 6. A simulation of the switch voltage and current produced by the circuit, shown in Fig. 5, using the device model for lock-on described in the text.

Figure 7. Switch voltage and current waveforms measured during a test of the circuit, shown in Fig. 5, when the switch was triggered with a 10-ns wide laser pulse at 532 nm. The voltage waveform shows that the switch can indeed stand off high voltage after recovering from lock-on. The current waveform indicates that the switch actually recovers in about 30 ns.

Figure 8. A comparison of lock-on with and without recovery. This figure shows the voltages delivered to the load, in the circuit of Fig. 5, for shots triggering the switch with different laser energies. Both shots used 532-nm laser pulses which were 10-ns wide. Above 1.4 mJ, the switch recovered rapidly from lock-on. At 1.4 mJ and lower, the switch stayed on until the energy in the circuit had dissipated.

Figure 9. Similar to Fig. 8, this figure shows a higher time resolution voltage waveform for a switch triggered with different laser

energies. Very little difference is indicated in these waveforms until the one triggered at 1.5 mJ starts to recover.

Figure 10. The circuit used to induce recovery from lock-on by limiting the current through the switch with a transmission line in series with the load. When the line is charged, current flow through the first switch stops. The second switch serves to discharge the line, restore the voltage across the first switch, and produce a pulse of the opposite polarity on the load.

Figure 11. A simulation of the switch voltage, produced by the circuit shown in Fig. 10, using the device model for lock-on described in the text. The two switches should produce a 12-MHz train of square pulses at voltages well above lock-on, 13 kV.

Figure 12. The circuit used to induce recovery from lock-on by limiting the current through the switch with an inductor after it has discharged a fast storage line.

Figure 13. A simulation of the switch, load, and inductor voltage for the circuit, shown in Fig. 12, using the device model for lock-on described in the text. Recovery depends on the size of the inductor, as given in relation 7.

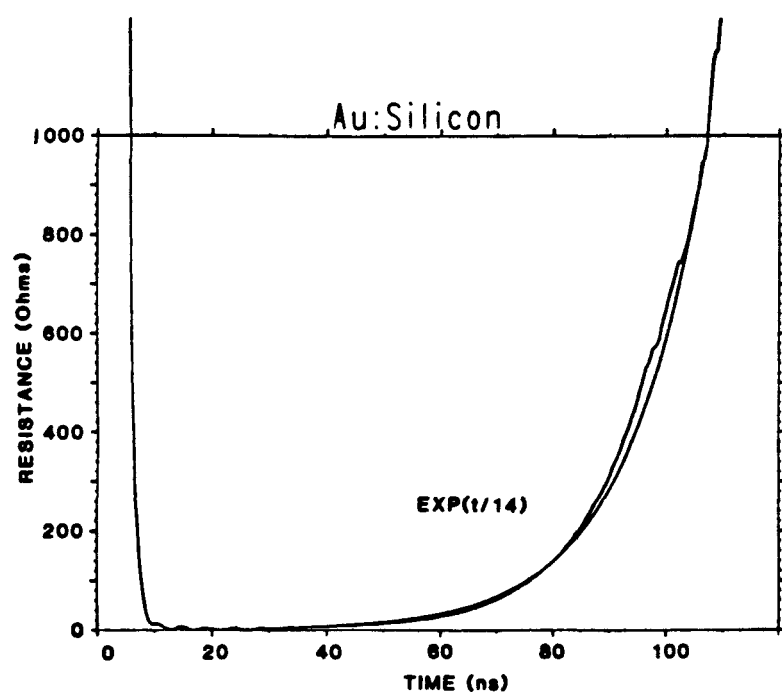


fig. 1

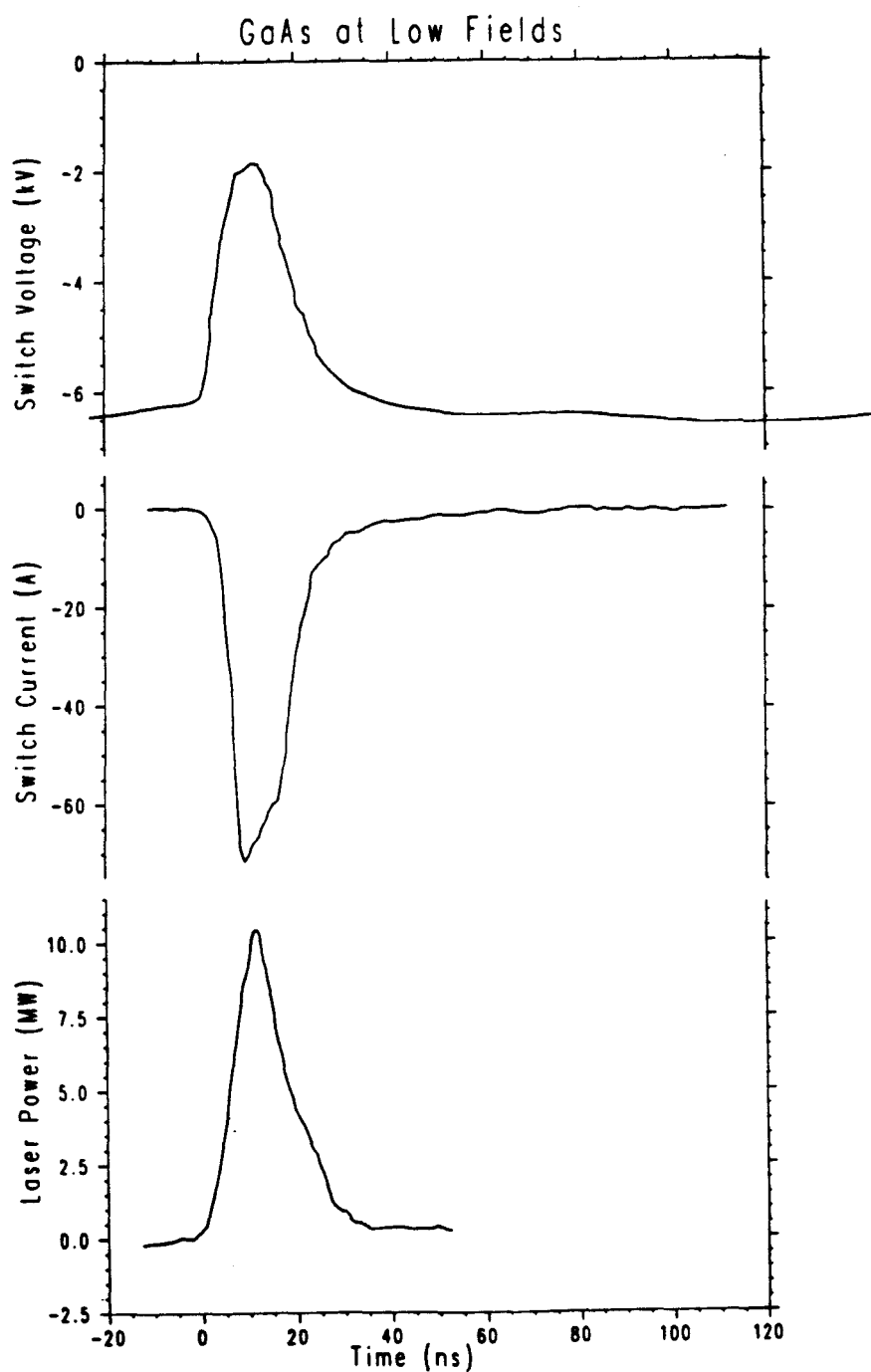


fig. 2

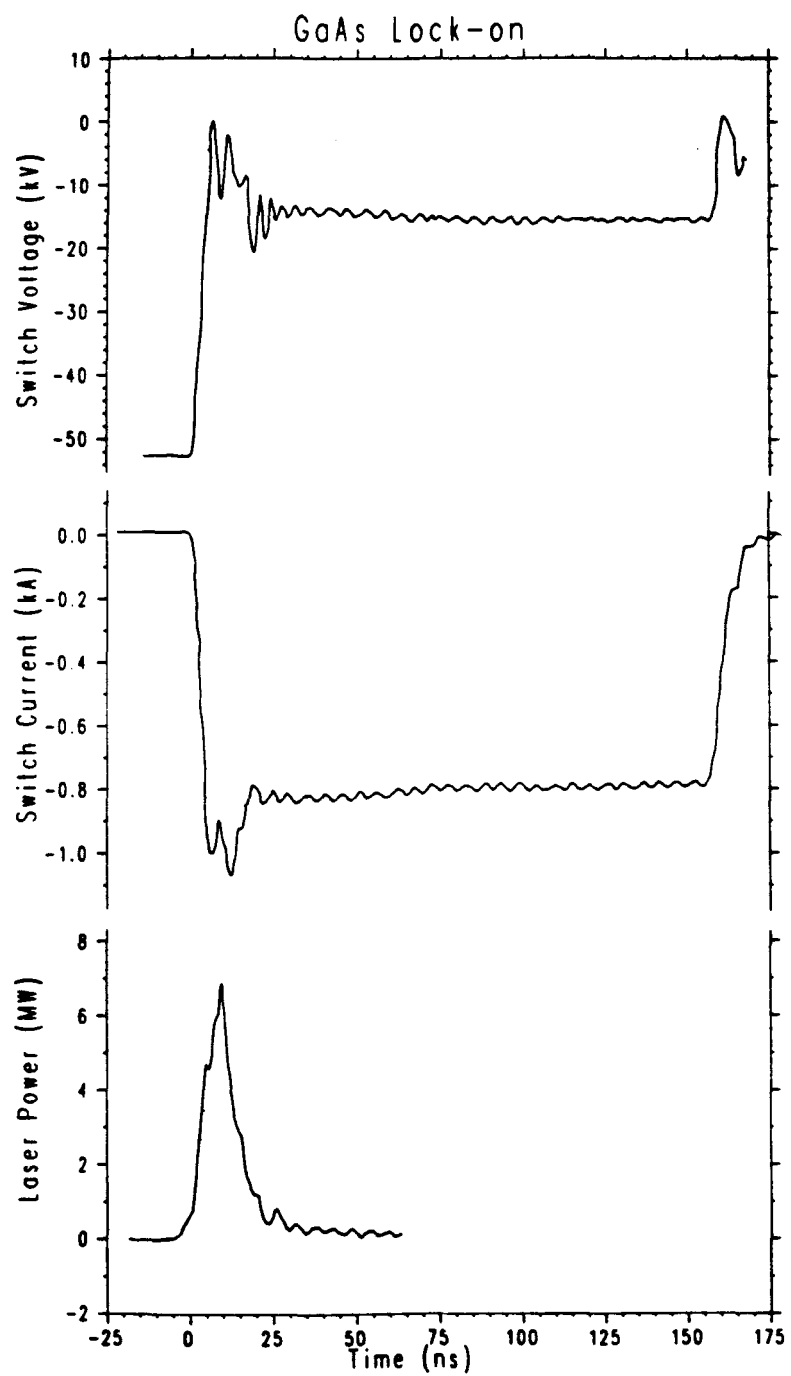


fig. 3

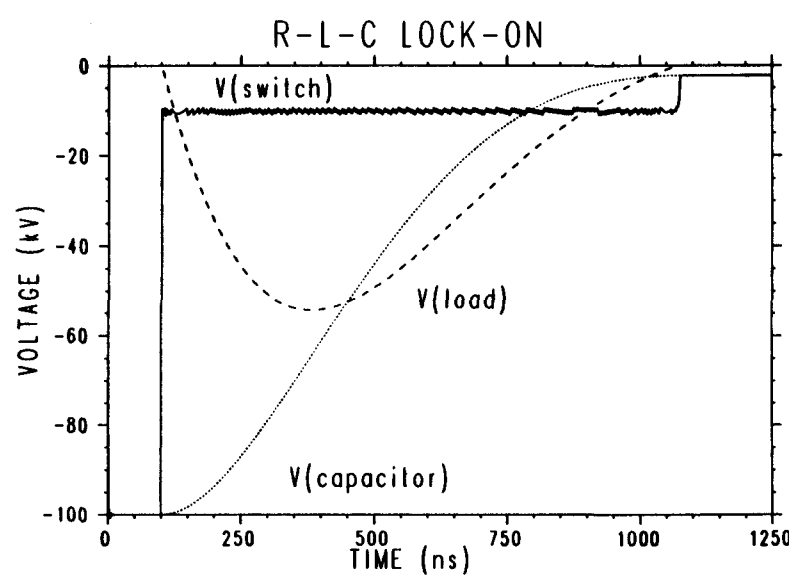


fig 4

## PARALLEL LOCK-ON CIRCUIT

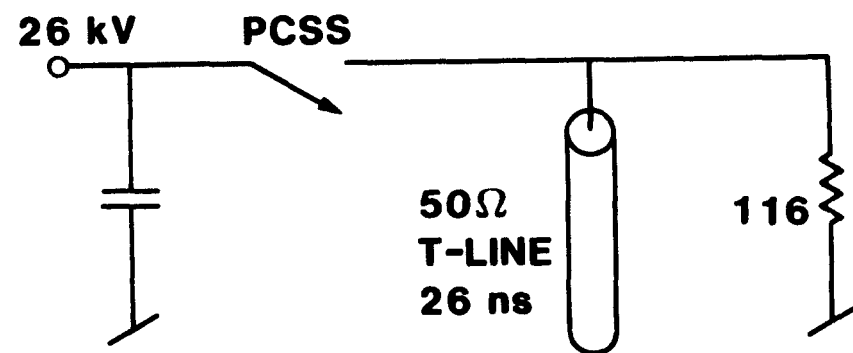


figure 5.

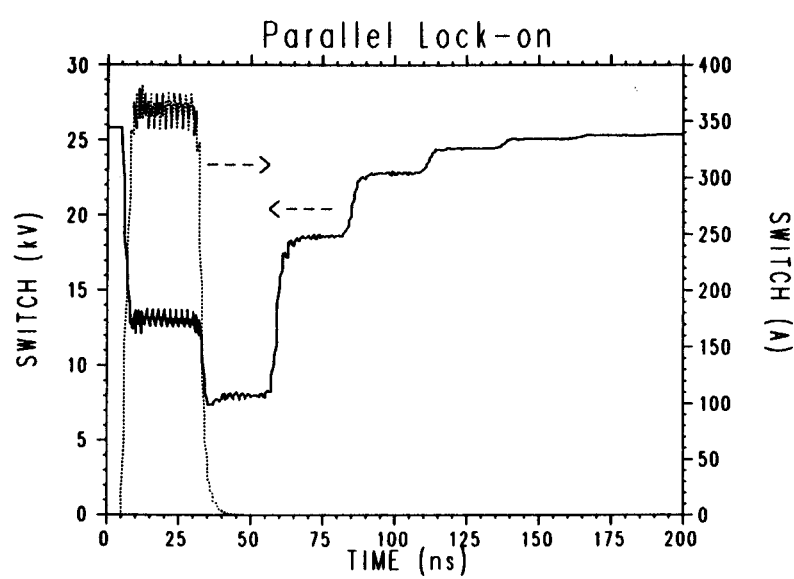


Fig. 6

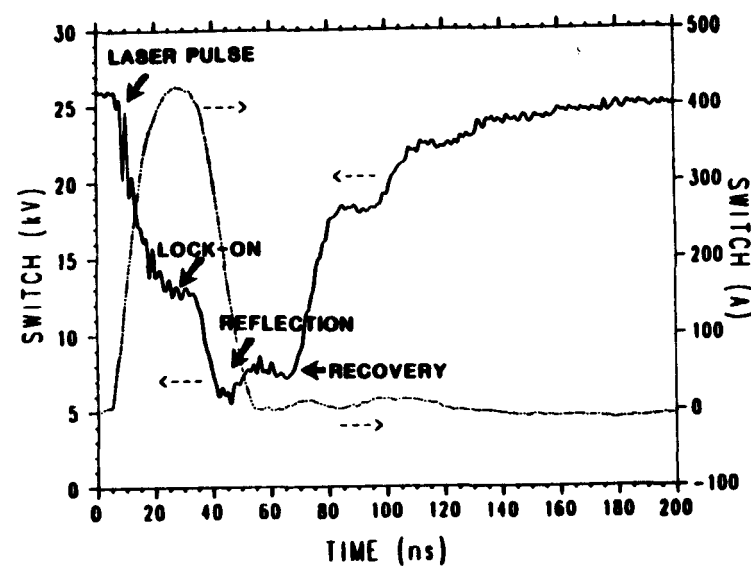


figure 7.

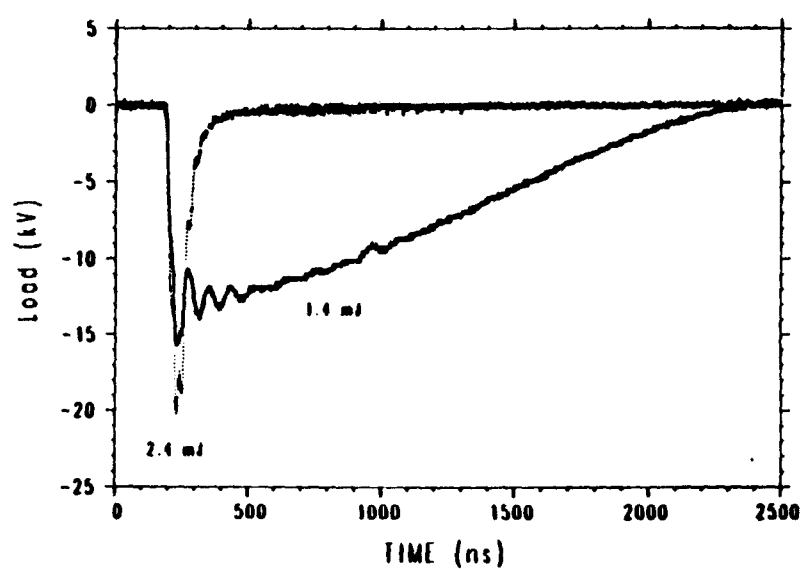


figure 8

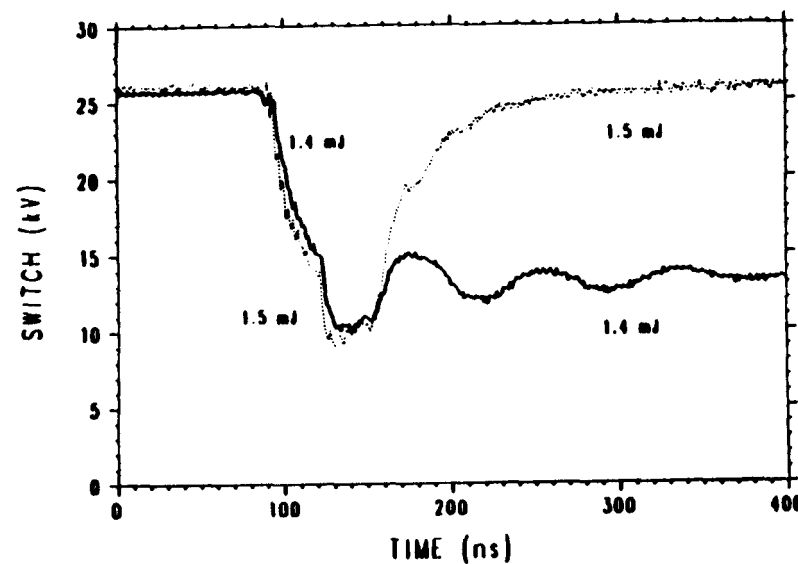


Figure 9.

## SERIES LOCK-ON CIRCUIT

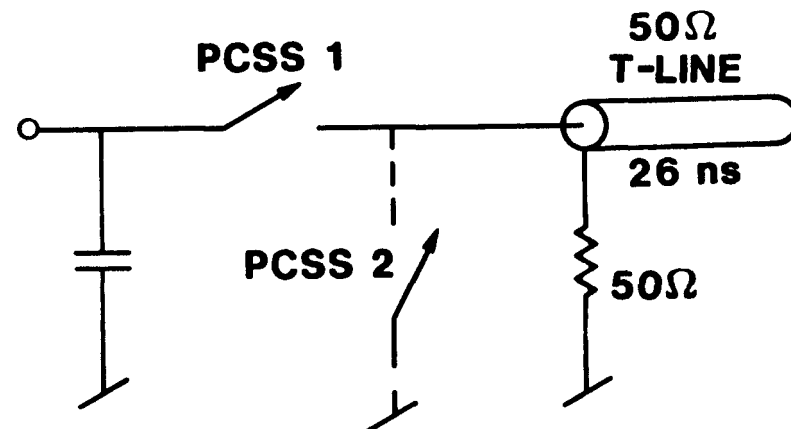


figure 10.

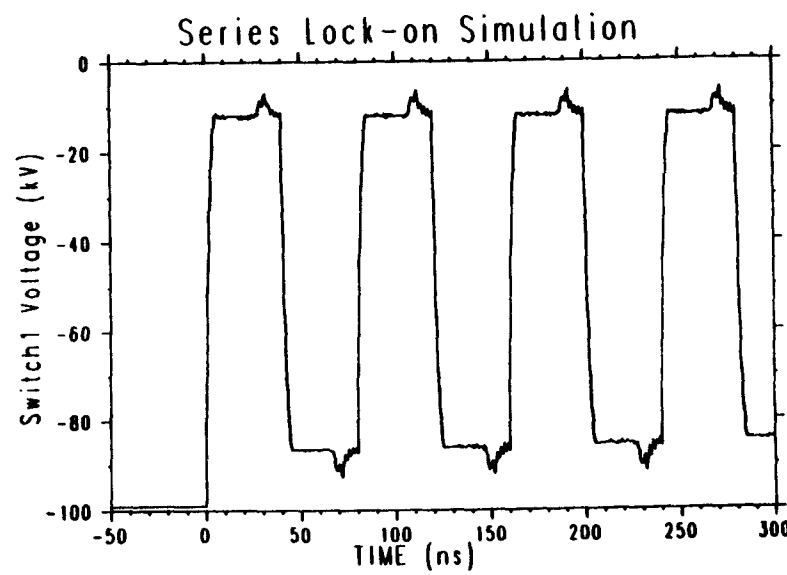


Figure 11.

## INDUCTIVELY LIMITED RECOVERY

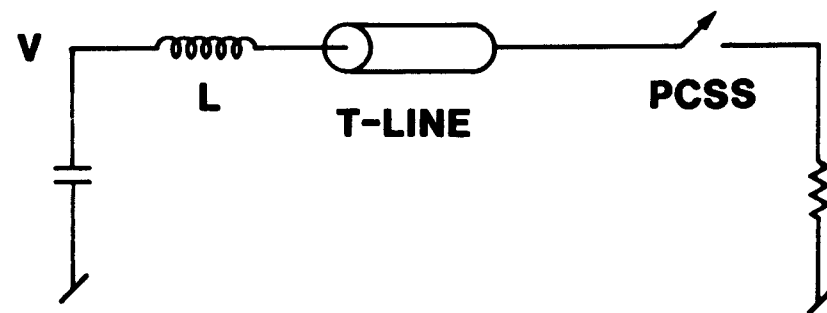


figure 12.

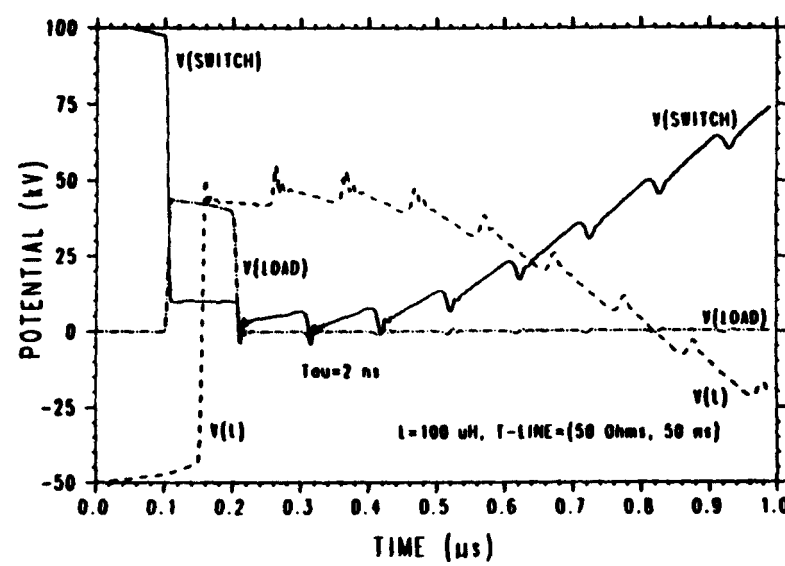


figure 13